

# New Experimental Limits on the Probabilities of Pauli-Forbidden Transitions in the $^{12}\text{C}$ Nucleus from Data Obtained with the Borexino Detector

A. V. Derbin<sup>\*1)</sup> and K. A. Fomenko<sup>\*\*2)</sup>  
(On behalf of the Borexino Collaboration<sup>3)</sup>)

Received March 23, 2010; in final form, May 31, 2010

**Abstract**—The Pauli exclusion principle was tested for nucleons in the  $^{12}\text{C}$  nucleus by using data from the Borexino detector. The approach used consisted in seeking photons, neutrons, and protons, as well as electrons and positrons, emitted in the Pauli-forbidden transitions of nucleons from the  $1P_{3/2}$  shell to the filled  $1S_{1/2}$  shell. Owing to a uniquely low background level in the Borexino detector and its large mass, the currently most stringent experimental limits were obtained for the probabilities and relative intensities of Pauli-forbidden transitions for the electromagnetic, strong, and weak channels.

DOI: 10.1134/S1063778810120112

## 1. INTRODUCTION

In the original form, the exclusion principle formulated by Pauli in 1925 postulates that the existence of two or more equivalent electrons in an atom is impossible [1]. Within quantum mechanics, the Pauli exclusion principle was formulated later on in the form of the requirement that the wave function describing a system of electrons be antisymmetric with respect to their permutations. In quantum field theory, the Pauli exclusion principle arises automatically for a

system of identical fermions as a consequence of the fact that fermion creation and annihilation operators satisfy anticommutation relations.

Despite the fundamental importance of the Pauli exclusion principle, physical reasons behind it have yet to be understood conclusively. According to L.B. Okun, “the nonconformist approach to the Pauli exclusion principle ... dates back to P. Dirac and E. Fermi” [2]: in the 1930s, both Dirac and Fermi discussed a possible effect of a small violation of the Pauli exclusion principle on the properties of atoms and on transitions in them [3, 4]. Pioneering experiments devoted to searches for Pauli-forbidden transitions were performed by F. Reines and H.W. Sobel [5], who sought x-ray radiation in transitions of electrons in atoms from the  $L$  shell to the filled  $K$  shell, and by B.A. Logan and A. Ljubicic [6], who attempted to detect photons in Pauli-forbidden transitions of nucleons in nuclei.

In 1987–1991, theoretical models that admit a small amount of violation of the Pauli exclusion principle were proposed by A.Yu. Ignatiev and V.A. Kuzmin [7], O.W. Greenberg and R.N. Mohapatra [8–10], and Okun [11]. However, A.B. Govorkov [12] showed that even a small amount of violation of the Pauli exclusion principle in those models would lead to negative values for the probabilities of some processes. Moreover, R.D. Amado and H. Primakoff indicated in 1980 [13] that, within quantum mechanics, the transitions that were sought in the experiments reported in [5, 6] and which are accompanied by the violation of the Pauli exclusion

<sup>1)</sup>Petersburg Nuclear Physics Institute, Russian Academy of Sciences, Gatchina, 188300, Russia.

<sup>2)</sup>Joint Institute for Nuclear Research, Dubna, Moscow oblast, 1419890 Russia.

<sup>3)</sup>G. Bellini, J. Benziger, S. Bonetti, M. Buizza Avanzini, B. Caccianiga, L. Cadonati, F. Calaprice, C. Carraro, A. Chavarria, F. Dalnoki-Veress, D. D’Angelo, H. de Kerret, A. Derbin, A. Etenko, K. Fomenko, D. Franco, C. Galbiati, S. Gazzana, M. Giammarchi, M. Goeger-Neff, A. Goretti, C. Grieb, S. Hardy, Aldo Ianni, Andrea Ianni, M. Joyce, V. Kobaychev, G. Korga, D. Kryn, M. Laubenstein, M. Leung, T. Lewke, E. Litvinovich, B. Loer, P. Lombardi, L. Ludhova, I. Machulin, S. Manecki, W. Maneschg, G. Manuzio, F. Masetti, K. McCarty, Q. Meindl, E. Meroni, L. Miramonti, M. Misiaszek, D. Montanari, V. Muratova, L. Oberauer, M. Obolensky, F. Ortica, M. Pallavicini, L. Papp, L. Perasso, S. Perasso, A. Pocar, R. S. Raghavan, G. Ranucci, A. Razeto, P. Risso, A. Romani, D. Rountree, A. Sabelnikov, R. Saldanha, C. Salvo, S. Schönert, H. Simgen, M. Skorokhvatov, O. Smirnov, A. Sotnikov, S. Sukhotin, Y. Suvorov, R. Tartaglia, G. Testera, D. Vignaud, R. B. Vogelaar, F. von Feilitzsch, M. Wojcik, M. Wurm, O. Zaimidoroga, S. Zavatarelli, and G. Zuzel.

\*E-mail: derbin@pnpi.spb.ru

\*\*E-mail: fomenko@jinr.ru

principle are impossible even if the Pauli exclusion principle is violated.

At the present time, there is no acceptable theoretical formalism for describing the violation of the Pauli exclusion principle. In particular, it is impossible to measure the amount of violation of the Pauli exclusion principle by introducing a “small parameter,” as is done in describing  $P$  and  $CP$  violation or a nonconservation of the lepton ( $L$ ) or baryon ( $B$ ) number. The results of relevant experiments are represented as limits on the lifetimes of atoms or nuclei with respect to forbidden transitions or as limits on the ratio of the rates of ordinary and Pauli-forbidden transitions. A critical analysis of theoretical and experimental problems concerning the possible violation of the Pauli exclusion principle was given in [2, 14, 15]. Original results of experiments devoted to testing the Pauli exclusion principle are presented in [16–49].

The most stringent limits on the probabilities of Pauli-forbidden transitions in the  $^{12}\text{C}$  nucleus that are accompanied by the emission of  $\gamma$ ,  $p$ ,  $n$ ,  $\alpha$ , and  $\beta^\pm$  particles were obtained with the Borexino detector prototype CTF (Counting Test Facility) [50]. In this article, we present new results obtained from the Borexino detector within 485 days of data taking [51]. The scintillator mass in the Borexino detector is 70 times as large as the scintillator mass in its CTF prototype, and the specific background level at the energy of 2 MeV is 200 times lower in the former than in the latter case. As a result, the limits on the probabilities for Pauli-forbidden transitions in the  $^{12}\text{C}$  nucleus were improved by three to four orders of magnitude.

## 2. BRIEF DESCRIPTION OF THE BOREXINO DETECTOR

Borexino is a real-time detector. It is deployed at the Gran Sasso underground laboratory (Italy). Measurement of the spectrum of low-energy solar neutrinos by detecting events of  $(\nu, e)$  scattering in a scintillator medium is the main task of the Borexino experiment. A uniquely high degree of purification of the detector from natural radioactivity and its large mass make it possible to solve other fundamental problems of particle physics and astrophysics along with addressing the above main task.

The basic properties of the detector were described in detail elsewhere [52–55]. The central volume of the detector is filled with 278 t of a scintillator based on pseudocumene (PC,  $\text{C}_9\text{H}_{12}$ ) supplemented with 1.5 g/l of PPO ( $\text{C}_{15}\text{H}_{11}\text{NO}$ ). The scintillator is contained in a thin-wall nylon vessel of a spherical shape—it is its inner volume (IV)—and is surrounded by two concentric buffer zones (323 and 567 t in mass) of pseudocumene supplemented with a small

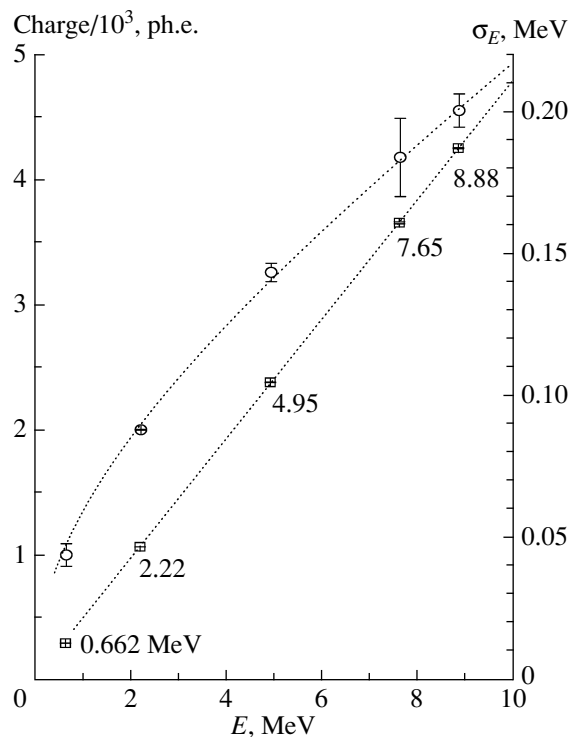


**Fig. 1.** Photon-energy dependence of the detected charge ( $\square$ , left-hand scale) and corresponding energy resolution  $\sigma_E$  ( $\circ$ , right-hand scale).

amount of quencher (dimethyl phthalate) in order to reduce scintillations. The buffer zones are separated by a nylon membrane intended for preventing radon diffusion. The inner volume and the buffer are placed within a steel sphere (SS) 13.7 m in diameter, and 2212 photomultiplier tubes (PMT) detecting scintillation light are arranged uniformly at the surface of this sphere. The steel sphere is placed in a domelike water tank (WT) 18.0 m in diameter and 16.9 m in height filled with 2100 t of ultrapure water, which serves as a shield from external neutrons and gamma rays. The detector structure materials were chosen in accordance with strict criteria of radiation purity. Another 208 photomultiplier tubes arranged within the water tank make it possible to detect Cherenkov light from passing muons.

The event energy is measured by the amount of light collected by all photomultiplier tubes. For a first approximation, the coefficient of proportionality between the amount of scintillation light and the event energy (light output) is taken to be independent of energy. The deviation from the linear dependence at low energies can be taken into account by introducing the ionization-deficiency (quenching) function  $f(k_B, E)$ , which depends on the Birks empirical constant  $k_B$  [56].

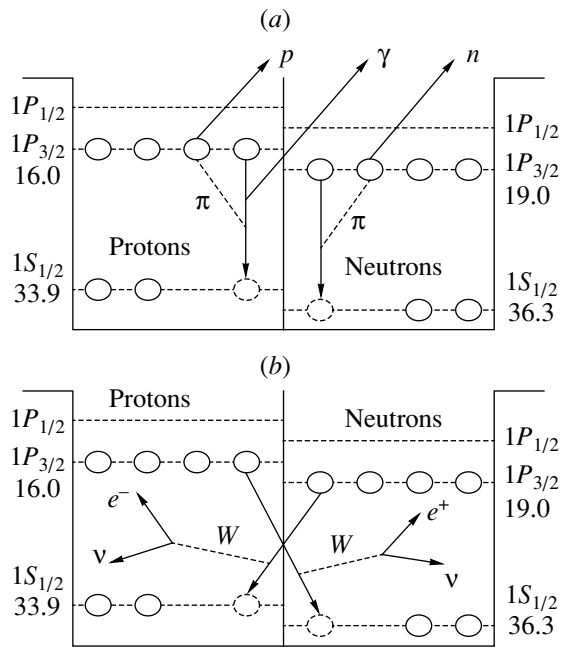


**Fig. 2.** Proton and neutron populations of the energy levels of the  $^{12}\text{C}$  nucleus in a simple shell model: schemes of Pauli-forbidden transitions of nucleons from the  $P$  shell to the filled  $S$  shell that are accompanied by the emission of (a)  $\gamma$ ,  $n$ ,  $p$ , and  $\alpha$  particles and (b)  $\beta^+$  and  $\beta^-$  particles (the energy is measured in MeV units).

The spatial and energy resolutions of the detector were studied with the aid of radioactive sources placed at various points within the inner volume. For energies above 2 MeV, which are of interest from the point of view of searches for transitions forbidden by the Pauli exclusion principle, the calibration was performed with a  $^{241}\text{Am}^9\text{Be}$  neutron source. The energy resolution behaves as  $\sigma_E/E \simeq (0.058 + 1.1 \times 10^{-3}E)/\sqrt{E}$ , where the energy  $E$  is taken in MeV units (see Fig. 1). Event coordinates were determined by the arrival time for signals from individual photomultiplier tubes. The detector spatial resolution

**Table 1.** Values of  $Q$  in Pauli-forbidden transitions (three neutrons or three protons in the  $S$  shell)

Channel	$Q_{3p}$ , MeV	$Q_{3n}$ , MeV
$^{12}\text{C} \rightarrow ^{12}\tilde{\text{C}} + \gamma$	$17.9 \pm 0.9$	$17.7 \pm 0.6$
$^{12}\text{C} \rightarrow ^{11}\tilde{\text{B}} + p$	$6.3 \pm 0.9$	$7.8 \pm 1.0$
$^{12}\text{C} \rightarrow ^{11}\tilde{\text{C}} + n$	$6.5 \pm 0.9$	$4.5 \pm 0.6$
$^{12}\text{C} \rightarrow ^8\tilde{\text{Be}} + \alpha$	$3.0 \pm 0.6$	$2.9 \pm 0.9$
$^{12}\text{C} \rightarrow ^{12}\tilde{\text{N}} + e^- + \bar{\nu}_e$	$18.9 \pm 0.9$	—
$^{12}\text{C} \rightarrow ^{12}\tilde{\text{B}} + e^+ + \nu_e$	—	$17.8 \pm 0.9$

determined for successive  $^{214}\text{Bi}$ – $^{214}\text{Po}$  events was  $13 \pm 2$  cm along the  $x$  and  $y$  axes and  $14 \pm 2$  cm along the  $z$  axis.

### 3. DATA ANALYSIS

#### 3.1. Theoretical Consideration

The scheme of energy levels of the  $^{12}\text{C}$  nucleus within a simple shell model is shown in Fig. 2. A transition of a nucleon from the  $P$  shell to the filled  $S$  shell leads to the formation of an excited Pauli-forbidden nucleus  $^{12}\tilde{\text{C}}$ . Its excitation energy is equal to the difference of the binding energies of nucleons in the  $S$  and  $P$  shells and is commensurate with the energies of proton, neutron, and alpha-particle separation ( $S_p$ ,  $S_n$ , and  $S_\alpha$ , respectively). Thus,  $n$ ,  $p$ , and  $\alpha$  particles can be emitted in addition to photons. In the present study, we also consider Pauli-forbidden weak processes such as the  $\beta^+$  and  $\beta^-$  transitions of nucleons to the filled  $1S_{1/2}$  shell (see Fig. 1).

The energy deposited in the transitions being considered is equal to the difference of the binding energies of the initial and final nuclei; that is,

$$Q(^{12}\text{C} \rightarrow \tilde{X} + Y) = M(^{12}\text{C}) - M(\tilde{X}) - M(Y) = -E_b(^{12}\text{C}) + E_b(\tilde{X}) + E_b(Y), \quad (1)$$

where  $\tilde{X}$  is a nuclear state forbidden by the Pauli exclusion principle;  $Y = \gamma, p, n, d, \alpha \dots$  are the emitted particles; and  $E_b$  stands for the corresponding binding energies, which are well known for ordinary nuclei [57]. A peak appearing in the observed spectrum and having a width that corresponds to the energy resolution of the detector is a signature of Pauli-forbidden transitions where there are two particles in the final state.

In the case of  $\beta^\pm$  transitions forbidden by the Pauli exclusion principle, a  $\beta^\pm$  spectrum must be observed. The endpoint energy of the  $\beta$  spectrum for the decay  $^{12}\text{C} \rightarrow ^{12}\tilde{\text{N}} + e^- + \bar{\nu}$  is given by

$$Q = m_n - m_p - m_e - E_b(^{12}\text{C}) + E_b(^{12}\tilde{\text{N}}). \quad (2)$$

A similar expression can be obtained for Pauli-forbidden transitions accompanied by positron emission, but the detected energy will be shifted by about  $2m_e$  because of the detection of two photons from the annihilation process.

The binding energy of the Pauli-forbidden nucleus involving three protons or three neutrons in the  $1S_{1/2}$  shell,  $E_b(\tilde{X})$ , can be estimated by using the binding energy of the respective ordinary nucleus,  $E_b(X)$ , and the difference of the nucleon binding energy in the

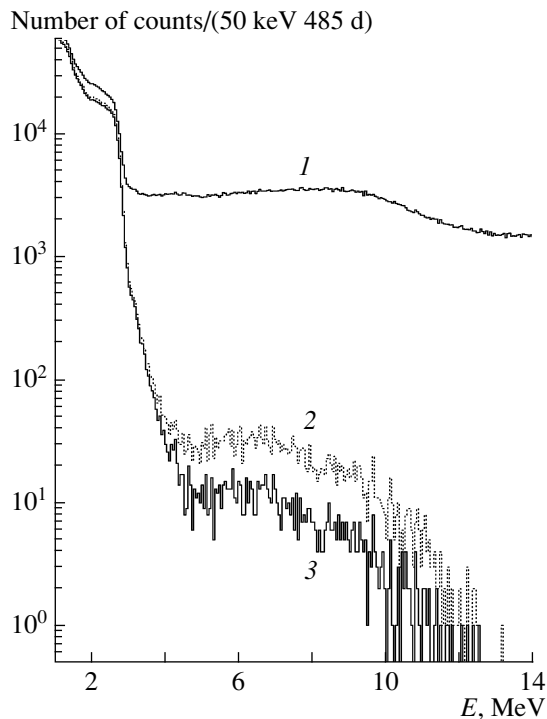


**Fig. 3.** Energy spectra of the Borexino detector: (1) spectrum of all detected events, (2) spectrum upon the subtraction of events in the interval of 2 ms after the passage of each muon, and (3) spectrum upon the subtraction of events in the interval of 0.7 s after the passage of muons that traversed the steel sphere.

$1S_{1/2}$  shell,  $E_{n,p}(1S_{1/2})$ , and the energy of nucleon separation from the outer shell,  $S_{n,p}(X)$ ; that is,

$$E_b(\tilde{X}_{n,p}) \simeq E_b(X) + E_{n,p}(1S_{1/2}) - S_{n,p}(X). \quad (3)$$

The binding energies of light nuclei ( $^{12}\text{C}$ ,  $^{11}\text{B}$ , and so on) were measured in studying the respective ( $p, 2p$ ) and ( $p, np$ ) reactions for protons of energy 1 GeV at the synchrocyclotron of the Petersburg Nuclear Physics Institute (PNPI) [58]. By using those data, we have calculated  $Q$  values (with errors) for various transitions forbidden by the Pauli exclusion principle that are presented in Table 1. The details of those calculations can be found in [50].

For the remaining reactions, such as  $^{12}\text{C} \rightarrow ^{10}\tilde{\text{B}} + d$ ,  $^{12}\text{C} \rightarrow ^9\tilde{\text{B}} + t$ ,  $^{12}\text{C} \rightarrow ^9\tilde{\text{Be}} + ^3\text{He}$ ,  $^{12}\text{C} \rightarrow ^6\tilde{\text{Li}} + ^6\text{Li}$ , and  $^{12}\text{C} \rightarrow ^6\tilde{\text{Li}} + ^4\text{He} + d$ , with the exception of  $^{12}\text{C} \rightarrow ^9\tilde{\text{B}}_{3p} + t$ ,  $Q$  values are negative. These reactions cannot be initiated by transitions forbidden by the Pauli exclusion principle.

By using the values obtained for  $Q$ , one can simulate the detector response functions for the reactions quoted in Table 1. In the present study, we have obtained a limit on the lifetime of  $^{12}\text{C}$  nuclei with respect to Pauli-forbidden transitions for each channel

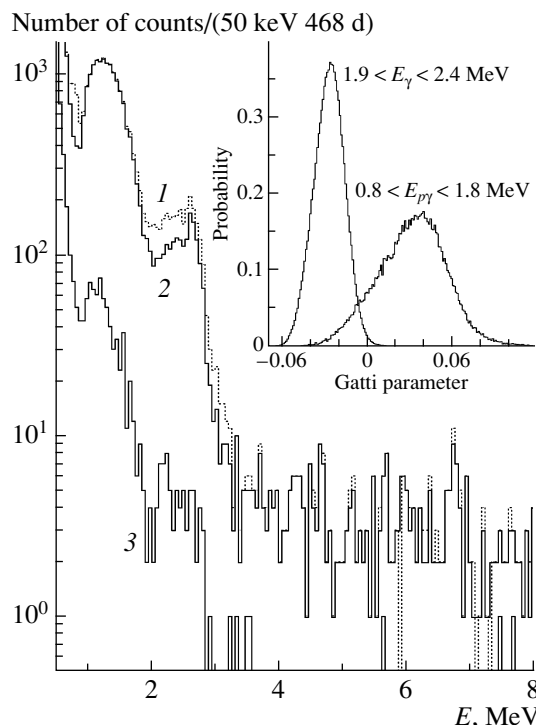


**Fig. 4.** Spectra of events detected within the  $R \leq 3.02$  m volume: (1) spectrum upon the subtraction of events in the intervals of 2 ms and 0.7 s after the passage of muons, (2) spectrum obtained after the removal of a pair of correlated events in the interval  $\Delta t \leq 2$  ms, and (3) spectrum obtained under the condition requiring that the Gatti variable be positive. The inset shows values of the Gatti variable that were obtained with a  $^{241}\text{Am}^9\text{Be}$  source for protons and photons of energy 2.2 MeV.

individually. Our results are compared with the rates of the corresponding normal transitions.

### 3.2. Selection of Data

Figure 3 shows the experimental spectrum of events that were obtained at Borexino in the energy range 1.0–14 MeV over 485 d of data taking (“live” time). Spectrum 1 corresponds to all detected events. At energies below 3 MeV, the detector background is determined by 2.6-MeV photons originating from the decay of  $^{208}\text{Tl}$  from the chain of decays of  $^{232}\text{Th}$  contained in the steel sphere and in photomultiplier tubes.

Spectrum 2 was obtained upon the subtraction of events detected within the time gate of width 2 ms after the muonic-veto signal. Moreover, the following additional requirements were imposed: the average time of arrival of signals from the photomultiplier tubes with respect to the time of actuation of the first photomultiplier tube in an event must not be longer than 100 ns, and the time corresponding to the maximum density of signals from the photomultiplier

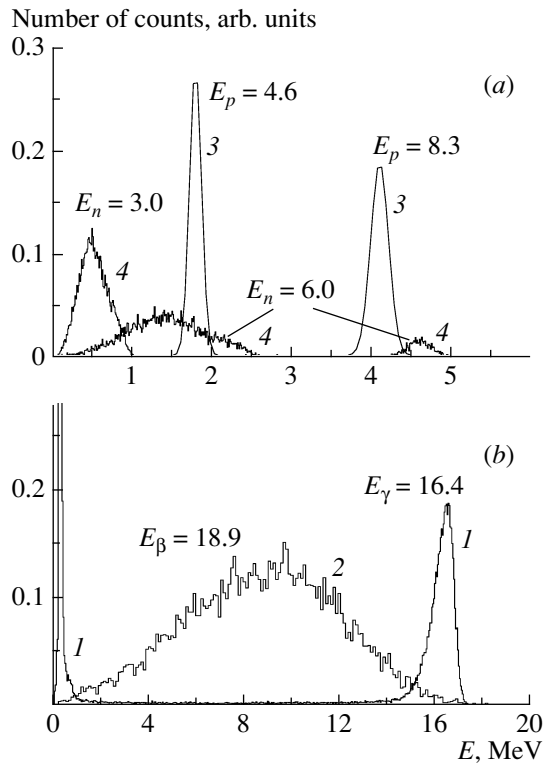


**Fig. 5.** Borexino detector response function for (1)  $^{12}\text{C} \rightarrow ^{12}\tilde{\text{C}} + \gamma$  (16.4 MeV), the inner volume and 1 m of the adjacent buffer; (2)  $^{12}\text{C} \rightarrow ^{12}\tilde{\text{N}} + e^- + \bar{\nu}$  (18.9 MeV); (3)  $^{12}\text{C} \rightarrow ^{11}\tilde{\text{B}} + p$  (4.6 and 8.3 MeV); and (4)  $^{12}\text{C} \rightarrow ^{11}\tilde{\text{C}} + n$  (3.0 and 6.0 MeV).

tubes in an event must not be longer than 30 ns. These selections remove events initiated by muons that traversed the steel sphere and which escaped detection in the outer Cherenkov detector.

In order to reduce the background from short-lived isotopes produced by muons ( $^9\text{Li}$  of half-life 178 ms and  $^8\text{He}$  of half-life 119 ms), events in the interval of 0.7 s after each muon that traversed the steel sphere were removed (spectrum 3 in Fig. 3). This selection reduced the “live” time to 467.8 d. The resulting spectrum features no event with an energy above 12.5 MeV. This fact will be used to set limits on Pauli-forbidden  $\beta^\pm$  transitions and transitions involving photon emission and having large  $Q$  values (see Table 1).

The energy spectrum in the range 0.5–8.0 MeV was studied in order to seek transitions forbidden by the Pauli exclusion principle that involve nucleon emission. Events detected in the scintillator central part of mass 100 t ( $R \leq 3.02$  m) were selected in order to reduce the external background (Fig. 4, spectrum 1). For this part of the detector, the background at energies below 3 MeV is approximately  $10^2$  times smaller than that for the entire volume. The

background level in the energy range between 1 and 2 MeV is determined by the  $\beta^+$  decay of the isotope  $^{11}\text{C}$ , which has a cosmic origin.

The next stage of the data analysis involved removing correlated events detected in the interval of 2 ms (spectrum 2 in Fig. 4). This leads primarily to the elimination of sequential  $^{214}\text{Bi}$ — $^{214}\text{Po}$  decays from the  $^{238}\text{U}$  family. Finally, a signal-shape selection criterion based on the Gatti filter [59] was applied to separate signals from electrons, protons and alpha particles. Spectrum 3 in Fig. 4 corresponds to proton- or alpha-particle-induced events for which the Gatti variable is positive (for more details, see [55]).

## 4. RESULTS

### 4.1. Limit on the Probability of Transitions Forbidden by the Pauli Exclusion Principle and Accompanied by Photon Emission: $^{12}\text{C} \rightarrow ^{12}\tilde{\text{C}} + \gamma$

A limit on the probability of  $^{12}\text{C} \rightarrow ^{12}\tilde{\text{C}} + \gamma$  forbidden transitions, which violate the Pauli exclusion principle, relies on the experimentally confirmed fact that there are no events of energy above 12.5 MeV that do not correlate with a muonic-veto signal. A lower limit on the lifetime of the  $^{12}\text{C}$  nucleus with respect to Pauli-forbidden transitions of nucleons from the  $P$  shell to the filled  $1S_{1/2}$  shell was calculated by the formula

$$\tau \geq \varepsilon(\Delta E) \frac{N_N N_n T}{S_{\text{lim}}}, \quad (4)$$

where  $\varepsilon(\Delta E)$  is the event-detection efficiency in the energy range  $\Delta E$ ,  $N_N$  is the number of  $^{12}\text{C}$  nuclei,  $N_n$  is the number of nucleons ( $n$  and/or  $p$ ) that are contained in the nucleus under study and for which the Pauli-forbidden transition being considered is possible,  $T$  is the time of the measurements, and  $S_{\text{lim}}$  is an upper limit on the possible number of candidates detected in the energy range  $\Delta E$  at a chosen confidence level,

From the data in Table 1, it follows that the most probable energy of the photon emitted in the transition of a nucleon from the  $1P_{3/2}$  shell to the  $1S_{1/2}$  shell is about 17.8 MeV. Taking into account the error in  $Q$ , we find that the photon energy lies in the interval 16.4–19.4 MeV at a 90% confidence level. The photon detection efficiency was determined by the Monte Carlo method with the aid of the GEANT4 package. Photons were uniformly generated within the inner volume and in the buffer zone 1 m thick directly adjacent to the inner volume. The detector response function for photons of energy 16.4 MeV is shown in Fig. 5. The efficiency for the conservative value of  $E_\gamma = 16.4$  MeV is  $\varepsilon(\Delta E) = 0.50$ .

The number of  $^{12}\text{C}$  atoms in 533 t of pseudocumene (inner volume and 1 m of buffer) is  $N_N = 2.37 \times 10^{31}$ . The number of nucleons in the  $P$ -shell is  $N_n = 8$ , the total data-taking time is  $T = 1.282$  yr, and the upper limit on the number of possible candidates is  $S_{\text{lim}} = 2.44$  at a 90% confidence level (C.L.) in accordance with the standard approach [60]. The lower limit on the nucleon lifetime is

$$\begin{aligned} & \tau_\gamma(^{12}\text{C} \rightarrow ^{12}\tilde{\text{C}} + \gamma) \\ & \geq 5.0 \times 10^{31} \text{ yr (at a 90\% C.L.).} \end{aligned} \quad (5)$$

This result improves the limit obtained previously with the CTF detector [50] by more than four orders of magnitude [ $\tau_\gamma(^{12}\text{C} \rightarrow ^{12}\tilde{\text{C}} + \gamma) \geq 2.1 \times 10^{27}$  yr] and the limit established by the NEMO-2 Collaboration [44] by more than seven orders of magnitude [ $\tau_\gamma(^{12}\text{C} \rightarrow ^{12}\tilde{\text{C}} + \gamma) \geq 4.2 \times 10^{24}$  yr]. The limit in (5) is commensurate with the limit obtained with the Kamiokande detector for  $^{16}\text{O}$  nuclei:  $\tau_\gamma(^{16}\text{O} \rightarrow ^{16}\tilde{\text{O}} + \gamma) \geq 1.0 \times 10^{32}$  yr for photons of energy in the range 19–50 MeV [43].

The limit obtained in the Kamiokande experiment for  $\tau_\gamma$  can be rescaled into a limit on the total lifetime of the nucleon with respect to transitions forbidden by the Pauli exclusion principle. The result is  $\tau = \tau_\gamma \times \text{Br}(\gamma)$ , where  $\text{Br}(\gamma) = \Gamma_\gamma/\Gamma_{\text{tot}}$  is the branching ratio for the channel involving photon emission. The  $\text{Br}(\gamma)$  value calculated for  $^{16}\text{O}$  nuclei lies in the interval  $(2.7\text{--}10.4) \times 10^{-5}$  [43]. In contrast to Kamiokande, the Borexino experiment can directly observe transitions forbidden by the Pauli exclusion principle and accompanied by the emission of protons or neutrons.

#### 4.2. Limit on the Probabilities of Pauli-Forbidden Transitions Occurring in the $^{12}\text{C}$ Nucleus and Involving Proton Emission: $^{12}\text{C} \rightarrow ^{11}\tilde{\text{B}} + p$

With allowance for the energy of the recoil nucleus ( $^{11}\tilde{\text{B}}$ ), the proton energy lies in the interval 4.6–8.3 MeV (at a 90% confidence level; see Table 1). The response function for protons was obtained by the Monte Carlo method with allowance for the decrease in the light output for protons in relation to electrons (see Fig. 5). The Birks constant [56] was determined from the recoil-proton spectrum measured with a  $^{241}\text{Am}^9\text{Be}$  source. For protons of energy  $E_p = 4.6(8.3)$  MeV, the measured light output corresponds to the electron energy of  $E_e = 1.8(4.1)$  MeV. This means that one can observe a proton peak in the range 1.8–4.1 MeV with a probability of 90%. The uncertainty in the peak position exceeds considerably the energy resolution of the detector ( $\sigma_E \cong 80$  keV at  $E_e = 2$  MeV).

The spectrum of events for which the Gatti variable is positive (spectrum 3 in Fig. 4) and which corresponds to the detection of protons (or alpha particles) was approximated by the sum of a polynomial function, which described a continuous background, and a Gaussian function, which corresponded to proton detection. The Gaussian function was centered consecutively at different points of the interval 1.8–4.1 MeV. The respective fit yielded the value of  $S_{\text{lim}} = 19$  at a 90% confidence level. Taking into account the efficiency of the Gatti criterion,  $\varepsilon = 0.89$ , and using expression (4), we obtain the following lower limit on the nucleon lifetime for 100 t of pseudocumene:

$$\begin{aligned} & \tau_p(^{12}\text{C} \rightarrow ^{11}\tilde{\text{B}} + p) \\ & \geq 2.1 \times 10^{30} \text{ yr (at a 90\% C.L.).} \end{aligned} \quad (6)$$

The lower limit on the lifetime of the  $^{12}\text{C}$  nucleus differs from the limit on the nucleon lifetime in (6) by a factor of  $N_n = 8$ . The limit obtained for the lifetime of the  $^{12}\text{C}$  nucleus is five orders of magnitude larger than the limit found for the  $^{23}\text{Na}$  and  $^{127}\text{I}$  nuclei with the 300-kg NaI detector ELEGANTV  $\{\tau(^{23}\text{Na}, ^{127}\text{I} \rightarrow ^{22}\tilde{\text{Ne}}, ^{126}\tilde{\text{Te}} + p) \geq 1.7 \times 10^{25}$  yr (at a 90% confidence level) for the emission of protons with energies in the region  $E_p \geq 18$  MeV [45]] and with the 250-kg NaI detector DAMA/LIBRA  $\{\tau(^{23}\text{Na}, ^{127}\text{I} \rightarrow ^{22}\tilde{\text{Ne}}, ^{127}\tilde{\text{Te}} + p) \geq 1.9 \times 10^{25}$  yr (at a 90% confidence level) for the emission of protons with energies in the region  $E_p \geq 10$  MeV [35]].

The energy of alpha particles emitted in the reaction  $^{12}\text{C} \rightarrow ^8\tilde{\text{Be}} + \alpha$  lies in the interval 1.0–3.0 MeV. Because of the quenching of the light output at high ionization densities, this corresponds to the interval 70–250 keV on the energy scale for electrons. The energy of 70 keV is close to the lower detection threshold for Borexino. Therefore, searches for the alpha-particle channel were not performed on the basis of the Borexino data. Our limit obtained for this Pauli-forbidden transition from the analysis of the data from CTF, whose detection threshold is 20 keV, is  $\tau(^{12}\text{C} \rightarrow ^8\tilde{\text{Be}} + \alpha) \geq 6.1 \times 10^{23}$  yr (at a 90% confidence level).

#### 4.3. Limit on the Probability of Pauli-Forbidden Transitions Occurring in $^{12}\text{C}$ Nuclei and Involving Neutron Emission: $^{12}\text{C} \rightarrow ^{11}\tilde{\text{C}} + n$

The kinetic energy of the initial neutron lies in the interval 3.2–7.3 MeV (at a 90% confidence level). Neutrons are thermalized fast in a scintillator containing a large amount of hydrogen. The mean lifetime of neutrons in pseudocumene is  $\tau \cong 250$   $\mu\text{s}$ , whereupon a neutron is captured on a proton. Thermal-neutron capture on a proton,  $n + p \rightarrow d + \gamma$

(the channel cross section is 0.33 b), is accompanied by the emission of a 2.2-MeV photon. The cross section for capture on a  $^{12}\text{C}$  nucleus is  $\sigma_\gamma = 3.5$  mb ( $E_\gamma = 4.95$  MeV); therefore, the intensity of the peak at 4.95 MeV is about 1% of the intensity of the peak at 2.2 MeV. The response function for 3.0- and 6.0-MeV neutrons is presented in Fig. 5. If the neutron energy exceeds the energy of the first excited level of  $^{12}\text{C}$  (4.44 MeV), a peak associated with the detection of 4.4-MeV photons appears in the detector response function.

Searches for Pauli-forbidden transitions accompanied by neutron emission were performed within the entire scintillator volume via selecting correlated pair events: a fast signal from recoil protons and a delayed signal from 2.2-MeV photons within the gate of 1.25 ms ( $5\tau$ ). We restricted the energy of the first event from below as  $E \geq 0.5$  MeV, this corresponding to the minimum possible detected energy of a neutron. The energy of the second event was chosen in the broad interval  $1.0 \leq E \leq 2.4$  MeV in order to enhance the detection efficiency for 2.2-MeV photons at the scintillator boundary. At a rather high primary neutron energy, the distance between events must not exceed 2 m. In all, 52 pairs of candidate events were found. For the maximum number of pairs,  $N = 26$ , the energy of the first event falls within the ranges 0.6–2.3 and 4.3–5.0 MeV, this corresponding to the primary neutron energy of 6 MeV. Taking into account the probability of the appearance of a signal in these ranges ( $\varepsilon = 0.9$ ), the detection efficiency for photons of energy 2.2 MeV ( $\varepsilon = 0.96$ ), the total number of  $^{12}\text{C}$  atoms within the inner volume ( $N_N = 1.24 \times 10^{31}$ ), and the value of  $S_{\text{lim}} = 33$  at a 90% confidence level, we obtain

$$\begin{aligned} \tau_n(^{12}\text{C} \rightarrow ^{11}\tilde{\text{C}} + n) \\ \geq 3.4 \times 10^{30} \text{ yr (at a 90\% C.L.).} \end{aligned} \quad (7)$$

This result is eight orders of magnitude larger than the limit obtained in searches for neutrino radiation from natural lead:  $\tau(\text{Pb} \rightarrow \text{Pb} + n) \geq 2.1 \times 10^{22}$  yr (at a 68% confidence level)[47].

#### 4.4. Limits on the Probabilities for Pauli-Forbidden $\beta^\pm$ Transitions: $^{12}\text{C} \rightarrow ^{12}\tilde{\text{N}} + e^- + \bar{\nu}$ and $^{12}\text{C} \rightarrow ^{12}\tilde{\text{B}} + e^+ + \nu$

The energy deposited in the reaction  $^{12}\text{C} \rightarrow ^{12}\tilde{\text{N}} + e^- + \bar{\nu}$  lies in the range 16.4–21.4 MeV. The shape of the  $\beta^-$  spectrum for the most probable endpoint energy of 18.9 MeV is shown in Fig. 5 according to calculations by the Monte Carlo method for the whole scintillator volume. The limit on the probability of a  $\beta^-$  transition forbidden by the Pauli exclusion

principle is based on the fact that there are no events for which  $E_e \geq 12.5$  MeV. The detection efficiency determined by means of a simulation for  $\beta^-$  particles of energy in the region  $E_e > 12.5$  MeV is  $\varepsilon = 0.12$ . The limit on the lifetime of a neutron ( $N_n = 4$ ) in the  $^{12}\text{C}$  nucleus with respect to transitions violating the Pauli exclusion principle is

$$\begin{aligned} \tau_{\beta^-}(^{12}\text{C} \rightarrow ^{12}\tilde{\text{N}} + e^- + \bar{\nu}) \\ \geq 3.1 \times 10^{30} \text{ yr (at a 90\% C.L.).} \end{aligned} \quad (8)$$

This result is six orders of magnitude larger than the limit obtained by the NEMO-2 Collaboration:  $\tau(^{12}\text{C} \rightarrow ^{12}\tilde{\text{N}} + e^- + \bar{\nu}) \geq 3.1 \times 10^{24}$  yr (at a 90% confidence level)[44].

Data from the LSD detector [61], situated in a tunnel under Mont Blanc, make it possible to obtain a qualitative limit for the decay mode being considered. According to [48], only two events of energy in excess of 12 MeV were detected within 75 d of data taking with the detector of mass 7.2 t ( $3 \times 10^{29}$   $^{12}\text{C}$  nuclei). The lower limit obtained by means of expression (4) (with  $S_{\text{lim}} = 5.91$  at a 90% confidence level and  $\varepsilon(E \geq 12 \text{ MeV}) = 0.23$ ) is  $\tau(^{12}\text{C} \rightarrow ^{12}\tilde{\text{N}} + e^- + \bar{\nu}) \geq 9.5 \times 10^{27}$  yr (at a 90% confidence level).

The endpoint energy of the  $\beta^+$  spectrum is 16.8 MeV, but the spectrum is additionally shifted by 0.85 MeV toward high energies because of the detection of two photons from the annihilation process (Fig. 5). The detection efficiency for the transition  $^{12}\text{C} \rightarrow ^{12}\tilde{\text{B}} + e^+ + \nu$ , which is forbidden by the Pauli exclusion principle and which is accompanied by an energy deposition in excess of 12.5 MeV, is  $\varepsilon = 0.079$ . The lower limit on the lifetime of a proton in the  $^{12}\text{C}$  nucleus is

$$\begin{aligned} \tau_{\beta^+}(^{12}\text{C} \rightarrow ^{12}\tilde{\text{B}} + e^+ + \nu) \\ \geq 2.1 \times 10^{30} \text{ yr (at a 90\% C.L.).} \end{aligned} \quad (9)$$

The limit obtained by the NEMO-2 Collaboration is more lenient by six orders of magnitude:  $\tau(^{12}\text{C} \rightarrow ^{12}\tilde{\text{B}} + e^+ + \nu) \geq 2.6 \times 10^{24}$  yr (at a 90% confidence level)[44].

The limits obtained for the lifetimes of nucleons with respect to transitions forbidden by the Pauli exclusion principle are given in Table 2 along with results found previously. The limit from [35] is a limit on the lifetimes of the  $^{23}\text{Na}$  and  $^{127}\text{I}$  nuclei. All of the remaining limits were presented for nucleons for which Pauli-forbidden transitions are possible in principle.

**Table 2.** Limits on the nucleon lifetime with respect to Pauli-forbidden transitions from the Borexino experiment

Channel	$\tau_{\text{lim}}, \text{y}\Gamma$	
	Borexino (90% C.L.)	Previous result
$^{12}\text{C} \rightarrow ^{12}\tilde{\text{C}} + \gamma$	$5.0 \times 10^{31}$	$4.2 \times 10^{24} (^{12}\text{C})$ [44] $1.0 \times 10^{32} (^{16}\text{O})$ [43]
$^{12}\text{C} \rightarrow ^{11}\tilde{\text{B}} + p$	$8.9 \times 10^{29}$	$1.9 \times 10^{25} (^{23}\text{Na}, ^{127}\text{I})$ [35]
$^{12}\text{C} \rightarrow ^{11}\tilde{\text{C}} + n$	$3.4 \times 10^{30}$	$2.1 \times 10^{22} (\text{natPb})$ [47]
$^{12}\text{C} \rightarrow ^{12}\tilde{\text{N}} + e^- + \bar{\nu}_e$	$3.1 \times 10^{30}$	$9.5 \times 10^{27} (^{12}\text{C})$ [48, 61]
$^{12}\text{C} \rightarrow ^{12}\tilde{\text{B}} + e^+ + \nu_e$	$2.1 \times 10^{30}$	$2.6 \times 10^{24} (^{12}\text{C})$ [44]

**Table 3.** Upper limits on relative intensities of Pauli-forbidden and normal transitions

Decay	$\tilde{\lambda} (^{12}\text{C}), \text{s}^{-1}$	$\lambda (^{12}\text{C}), \text{s}^{-1}$	$\delta^2 = \tilde{\lambda}/\lambda$ (90% C.L.)	
			our study	previous result
$\gamma$	$5.0 \times 10^{-39}$	$2.3 \times 10^{18}$	$2.2 \times 10^{-57}$	$2.3 \times 10^{-57}$ [43]
$N_{n,p}$	$7.4 \times 10^{-38}$	$1.8 \times 10^{22}$	$4.1 \times 10^{-60}$	$3.5 \times 10^{-55}$ [35]
$(e, \nu)$	$4.1 \times 10^{-38}$	$2.0 \times 10^{-3}$	$2.1 \times 10^{-35}$	$6.5 \times 10^{-34}$ [48, 61]

#### 4.5. Limits on Relative Intensities of Transitions Forbidden by the Pauli Exclusion Principle

Transitions forbidden by the Pauli exclusion principle and accompanied by the emission of  $\gamma$ ,  $n$ , or  $p$  particles and  $(\nu, e)$  pairs may be caused by, respectively, electromagnetic, strong, and weak interactions. The lower limits obtained for the nucleon lifetime can be rescaled into limits on the ratio of intensities of Pauli-forbidden and normal transitions:  $\delta^2 = \tilde{\lambda}/\lambda$ , where  $\lambda = 1/\tau$  is the rate (intensity) of a forbidden ( $\tilde{\lambda}$ ) and a normal ( $\lambda$ ) transition. The ratio of the constants that determine the intensity of forbidden ( $g_{\text{PV}}$ ) and normal ( $g_{\text{NT}}$ ) transitions,  $\delta^2 = (g_{\text{PV}}/g_{\text{NT}})^2$ , can be used as a measure of violation of the Pauli exclusion principle and can be considered as a possible admixture of nonfermionic statistics. In particular, the parameter  $\delta^2 = \beta^2/2$  in the model of violation of the Pauli exclusion principle from [9, 10] corresponds to the square of the amplitude of the symmetric component of the fermion wave function. The use of the relative intensity of forbidden and normal transitions makes it possible to compare experimental limits obtained for the lifetimes of various atoms and nuclei.

The nuclear-level width associated with the 16.4-MeV  $E1$   $\gamma$  transition from the  $P$  shell to the  $S$  shell can be determined by the Weisskopf formula. The resulting value of  $\Gamma_\gamma \approx 1.5$  keV corresponds to the transition rate of  $\lambda = \Gamma_\gamma/\hbar = 2.3 \times 10^{18} \text{ s}^{-1}$ . For the lower limit on  $\tau_\gamma$  in (5), we obtain  $\delta_\gamma^2 = \tilde{\lambda} (^{12}\text{C})/\lambda (^{12}\text{C}) \leq 2.2 \times 10^{-57}$  (at a 90% confidence

level). This result is close to the limit obtained with the Kamiokande detector for  $^{16}\text{O}$  nuclei:  $\delta_\gamma^2 = 2.3 \times 10^{-57}$  [43].

Although  $E1$  transitions are the fastest among  $\gamma$  transitions, the level width associated with hadron emission is three to four orders of magnitude larger. As a result, a substantially more stringent limit on the relative intensity of transitions forbidden by the Pauli exclusion principle and accompanied by nucleon emission can be obtained in the case of equal limits on the lifetimes with respect to processes involving the emission of photons and nucleons. The width of the  $S$  level in the  $^{12}\text{C}$  nucleus is  $\Gamma_{n,p} \cong 12$  MeV according to measurements in the respective  $(p, 2p)$  and  $(p, pn)$  reactions [58]. The limit on  $\tau_p$  in (6) and the limit on  $\tau_n$  in (7) lead to the following constraints:  $\delta_p^2 = \tilde{\lambda}/\lambda \leq 1.6 \times 10^{-59}$  and  $\delta_n^2 \leq 4.1 \times 10^{-60}$  at a 90% confidence level. These results are four orders of magnitude more stringent than the limit established by the DAMA Collaboration [35].

Pauli-forbidden  $\beta^\pm$  transitions are first-order-forbidden  $P \rightarrow S$  transitions. For such transitions, the value of  $\log(F_{t_{1/2}})$  is  $7.5 \pm 1.5$ . The conservative value of  $\log(F_{t_{1/2}}) = 9$  corresponds to  $\tau \approx 480$  s at  $Q = 18.9$  MeV in the case of  $\beta^-$  decay (the level width is  $\Gamma_{\beta^-} \approx 1.4 \times 10^{-18}$  eV) and to  $\tau \approx 1050$  s at  $Q = 17.8$  MeV in the case of  $\beta^+$  decay. As a result, the limits on the relative intensity of  $\beta^\pm$  decays forbidden by the Pauli exclusion principle are considerably more lenient:  $\delta_{\beta^-}^2 \leq 2.1 \times 10^{-35}$  and



$\delta_{\beta^+}^2 \leq 6.4 \times 10^{-35}$  at a 90% confidence level. The existing constraint  $\delta_{\beta^-}^2 \leq 6.5 \times 10^{-34}$ , which was obtained in [48] with the aid of LSD data [61], is more lenient by a factor of 30. The limit on the relative intensity of  $\beta^\pm$  transitions is substantially more lenient than the limit for transitions involving nucleon and photon emission, but we would like to highlight a significant distinction between these processes. In  $\beta^\pm$  transitions, new particles ( $p$  or  $n$ ) appear. The Amado–Primakoff forbiddenness, which is valid only for a system of identical particles, cannot be applied to transitions in which the initial and final states are formed by different sets of particles [13, 48]. Thus, the limit on  $\delta_{\beta^\pm}^2$  can be compared with the limit obtained in the VIP experiment— $\beta^2/2 \leq 4.5 \times 10^{-28}$  [38].

The limits that we obtained for the relative intensities of transitions forbidden by the Pauli exclusion principle and for normal transitions are presented in Table 3.

## 5. CONCLUSIONS

The use of unique properties of the Borexino detector, such as an extremely low background level, a large scintillator mass, a low detection threshold, and an efficient system for the identification of muon-induced events, made it possible to obtain new, currently the most stringent, limits on the probabilities of the Pauli-forbidden transitions of nucleons from the  $1P_{3/2}$  shell to the  $1S_{1/2}$  shell in  $^{12}\text{C}$  nuclei with the emission of  $\gamma$ ,  $n$ ,  $p$ , and  $\beta^\pm$  particles; that is,

$$\begin{aligned}\tau(^{12}\text{C} \rightarrow ^{12}\tilde{\text{C}} + \gamma) &\geq 5.0 \times 10^{31} \text{ yr}, \\ \tau(^{12}\text{C} \rightarrow ^{11}\tilde{\text{B}} + p) &\geq 8.9 \times 10^{29} \text{ yr}, \\ \tau(^{12}\text{C} \rightarrow ^{11}\tilde{\text{C}} + n) &\geq 3.4 \times 10^{30} \text{ yr}, \\ \tau(^{12}\text{C} \rightarrow ^{12}\tilde{\text{N}} + e^- + \nu) &\geq 3.1 \times 10^{30} \text{ yr}, \\ \tau(^{12}\text{C} \rightarrow ^{12}\tilde{\text{B}} + e^+ + \bar{\nu}) &\geq 2.1 \times 10^{30} \text{ yr},\end{aligned}$$

the confidence level being 90% for all of these transitions.

The constraints that we obtained make it possible to set new upper limits on the relative intensities of transitions forbidden by the Pauli exclusion principle and normal transitions:  $\delta_\gamma^2 \leq 2.2 \times 10^{-57}$ ,  $\delta_N^2 \leq 4.1 \times 10^{-60}$ , and  $\delta_\beta^2 \leq 2.1 \times 10^{-35}$  (at a 90% confidence level).

## ACKNOWLEDGMENTS

The accomplishment of the research program of the Borexino experiment became possible owing to the financial support of INFN (Italy); NSF (USA); BMBF, DFG, and MPG (Germany); the Ministry

of Science of the Russian Federation; and MNiSW (Poland). The present authors gratefully acknowledge the generous and permanent support of Istituto Nazionale di Fisica Nucleare (INFN) and Laboratori Nazionali del Gran Sasso (LNGS). The work of A.V. Derbin was supported by Fondazione Cariplo.

## REFERENCES

1. W. Pauli, *Z. Phys.* **31**, 765 (1925).
2. L. B. Okun, *Usp. Fiz. Nauk* **158**, 293 (1989) [*Sov. Phys. Usp.* **32**, 543 (1989)].
3. P. A. M. Dirac, *The Principles of Quantum Mechanics* (Clarendon, Oxford, 1958), Chap. IX.
4. E. Fermi, *Scientia* **55**, 21 (1934).
5. F. Reines and H. W. Sobel, *Phys. Rev. Lett.* **32**, 954 (1974).
6. B. A. Logan and A. Ljubicic, *Phys. Rev. C* **20**, 1957 (1979).
7. A. Yu. Ignatiev and V. A. Kuz'min, *Yad. Fiz.* **46**, 1338 (1987) [*Sov. J. Nucl. Phys.* **46**, 786 (1987)]; hep-ex/0510209.
8. O. W. Greenberg and R. N. Mohapatra, *Phys. Rev. Lett.* **59**, 2507 (1987); *Phys. Rev. Lett.* **62**, 712 (1989); *Phys. Rev. D* **39**, 2032 (1989).
9. O. W. Greenberg, *Phys. Rev. Lett.* **64**, 705 (1990).
10. R. N. Mohapatra, *Phys. Lett. B* **242**, 407 (1990).
11. L. B. Okun, *JETP Lett.* **46**, 529 (1987).
12. A. B. Govorkov, *Phys. Lett. A* **137**, 7 (1989).
13. R. D. Amado and H. Primakoff, *Phys. Rev. C* **22**, 1338 (1980).
14. L. B. Okun, *Comm. Nucl. Part. Phys.* **19**, 99 (1989).
15. A. Yu. Ignatiev, hep-ph/0509258.
16. *Intern. Conf. on Spin Statistics Connection and Commutation Relations: Experimental Tests and Theoretical Implications, Anacapri, Napoli, Italy, 31 May–3 June 2000*, Ed. by R. C. Hilborn and G. M. Tino, AIP Conf. Proc. **545** (2000).
17. *Theoretical and Experimental Aspects of the Spin-Statistics Connection and Related Symmetries*, <http://www.ts.infn.it/eventi/spinstat2008/allTalks.php>
18. V. M. Novikov and A. A. Pomanskiĭ, *Pis'ma Zh. Éksp. Teor. Fiz.* **49**, 68 (1989) [*JETP Lett.* **49**, 81 (1989)].
19. V. M. Novikov et al., *Phys. Lett. B* **240**, 227 (1990).
20. E. Nolte et al., *Z. Phys. A* **340**, 411 (1991).
21. D. Javorsek et al., *Phys. Rev. Lett.* **85**, 2701 (2000).
22. A. S. Barabash et al., *JETP Lett.* **68**, 112 (1998).
23. E. Nolte et al., *Nucl. Instrum. Methods Phys. Res. B* **52**, 563 (1990).
24. G. Feinberg and M. Goldhaber, *Proc. Natl. Acad. Sci. USA* **45**, 1301 (1959).
25. M. K. Moe and F. Reines, *Phys. Rev. B* **140**, 992 (1965).
26. R. I. Steinberg et al., *Phys. Rev. D* **12**, 2582 (1975).
27. E. L. Kovalchuk, A. A. Pomanskiĭ, and A. A. Smol'nikov, *JETP Lett.* **29**, 145 (1979).
28. E. Bellotti et al., *Phys. Lett. B* **124**, 435 (1983).
29. F. T. Avignone III et al., *Phys. Rev. D* **34**, 97 (1986).
30. D. Reusser et al., *Phys. Lett. B* **255**, 143 (1991).

31. H. Ejiri et al., Phys. Lett. B **282**, 281 (1992).
32. Y. Aharonov et al., Phys. Lett. B **353**, 168 (1995).
33. P. Belli et al., Astropart. Phys. **5**, 217 (1996).
34. P. Belli et al., Phys. Lett. B **460**, 236 (1999).
35. R. Bernabei et al., Eur. Phys. J. C **62**, 327 (2009).
36. K. Akama, H. Terazawa, and M. Yasue, Phys. Rev. Lett. **68**, 1826 (1992).
37. E. Ramberg and G. A. Snow, Phys. Lett. B **238**, 438 (1990).
38. VIP Collab. (S. Bartalucci et al.), Phys. Lett. B **641**, 18 (2006); C. Curceanu Petrascu et al., arXiv:0803.0870[quant-ph].
39. K. Deilamian, J. D. Gillaspay and D. E. Kelleher, Phys. Rev. Lett. **74**, 4787 (1995).
40. R. C. Hilborn and C. L. Yuca, Phys. Rev. Lett. **76**, 2844 (1996).
41. M. de Angelis, G. Gagliardi, L. Gianfrani, and G. M. Tino, Phys. Rev. Lett. **76**, 2840 (1996).
42. G. Modugno, M. Inguscio, and G. M. Tino, Phys. Rev. Lett. **81**, 4790 (1998).
43. Y. Suzuki et al., Phys. Lett. B **311**, 357 (1993).
44. NEMO Collab. (R. Arnold et al.), Eur. Phys. J. A **6**, 361 (1999).
45. H. Ejiri and H. Toki, Phys. Lett. B **306**, 218 (1993).
46. R. Bernabei et al., Phys. Lett. B **408**, 439 (1997).
47. T. Kishimoto et al., J. Phys. G **18**, 443 (1992).
48. D. Kekez, A. A. Ljubičić, and B. A. Logan, Nature **348**, 224 (1990).
49. D. Miljanić et al., Phys. Lett. B **252**, 487 (1990).
50. Borexino Collab. (H. O. Back et al.), Eur. Phys. J. C **37**, 421 (2004).
51. Borexino Collab. (G. Bellini et al.), Phys. Rev. C **81**, 034317 (2010).
52. Borexino Collab. (G. Alimonti et al.), Astropart. Phys. **16**, 205 (2002).
53. Borexino Collab. (C. Arpesella et al.), Phys. Lett. B **568**, 101 (2008).
54. Borexino Collab. (C. Arpesella et al.), Phys. Rev. Lett. **101**, 091302 (2008).
55. Borexino Collab. (G. Alimonti et al.) Nucl. Instrum. Methods Phys. Res. A **600**, 568 (2009).
56. J. B. Birks, Proc. Phys. Soc. London, Sect. A **64**, 874 (1951).
57. G. Audi and A. H. Wapstra, Nucl. Phys. A **595**, 409 (1995).
58. S. L. Belostotskiĭ et al., Yad. Fiz. **41**, 1425 (1985) [Sov. J. Nucl. Phys. **41**, 903 (1985)].
59. E. Gatti and F. De Martini, in *Nuclear Electronics* (IAEA, Vienna, 1962), Vol. 2, p. 265.
60. G. J. Feldman and R. D. Cousins, Phys. Rev. D **57**, 3873 (1998).
61. M. Aglietta et al., Nuovo Cimento C **9**, 185 (1986).

*Translated by A. Isaakyan*